Chemical Engineering Journal 166 (2011) 428–434

Contents lists available at ScienceDirect

Chemical Engineering Journal

journal homepage: www.elsevier.com/locate/cej

Low temperature aqueous synthesis of highly dispersed Co_3O_4 nanocubes and their electrocatalytic activity studies

Yunling Li[a,b,c], Jingzhe Zhao[a,*], Yuanyuan Dan[b], Dechong Ma[a], Yan Zhao[a,b], Shengnan Hou[a], Haibo Lin[b,*], Zichen Wang[b]

[a] College of Chemistry and Chemical Engineering, Hunan University, Yuelu Mountain, Changsha 410082, PR China
[b] College of Chemistry, Jilin University, Changchun 130023, PR China
[c] College of Chemistry and Chemical Engineering, Hennan Institute of Science and Technology, PR China

ARTICLE INFO

Article history:
Received 26 April 2010
Received in revised form 19 October 2010
Accepted 30 October 2010

Keywords:
Co_3O_4 nanocubes
Aqueous solution
Dispersibility
Electrocatalytic materials

ABSTRACT

We report here a simple approach to the synthesis of highly dispersed Co_3O_4 nanocubes in higher yield by aqueous precipitation method at low temperatures (70–90 °C). The nanosized Co_3O_4 powders were directly achieved from Co(II) aqueous solution under alkaline and oxidizing conditions. TEM results indicate that the as-prepared Co_3O_4 has a cubic nanostructure with uniform size of about 20 nm and narrow size distribution. Powder X-ray diffraction (XRD) and infrared spectrum (IR) results show that the samples are Co_3O_4 in spinel structure. The objective Co_3O_4 nanocubes can be achieved in a wide range of experimental parameters, which can be preserved as stable suspension in distilled water or ethanol for several months with no obvious change. Appropriate reaction time and temperature should be controlled to get better crystallized Co_3O_4 nanocubes with perfect cubic appearance and good dispersibility. It is essential to achieve cubic-like Co_3O_4 particles by using ammonia as precipitator. The as-prepared Co_3O_4 nanocubes, combined with PbO_2 as electrodes, extend improved electrocatalytic activities and decreased oxygen evolution potential in electrochemical reactions, so they can be used as potential electrode materials or electrocatalytic materials. This facile method for the synthesis of Co_3O_4 nanocubes is a simple and general process without any seed, catalyst, or template, thus it is promising for large-scale and low-cost production of Co_3O_4 with high-quality.

1. Introduction

Over the past decades, nanoscale materials, on the development of nanoscience and nanotechnology, have attracted a great deal of interests from researchers owing to their shape/size-dependent properties [1–4]. Driven by the minimization of the surface energy, nanoscale solids tend to either grow into large particles or aggregate into large coalescences during their formation. To prevent these undesired processes and obtain highly dispersed nanomaterials, much research has been performed, such as employing surface modifying/stabilizing compounds in the constrained preparation or using soft colloidal templates to control the growth [5,6]. Research in this area is motivated by the possibility of designing nanostructured particles with uniform size and specific shape. Therefore, more research efforts were focused on increasing the dispersibility of nanoscale materials [7–10].

Transition-metal oxides in nanometer size display many interesting size dependent physical and chemical properties [11–14]. Among these oxides, Cobalt (II, III) oxide Co_3O_4, a p-type semiconductor ceramic material with a spinel crystal structure (Fd3m), is known as a promising material that exhibits a wide range of applications including catalyst, gas sensor, electrochromic device, solar energy absorber, and magnetic material [15–20]. There are growing interests to synthesize Co_3O_4 nanostructures with unique size and specific shape because of the influences of particle size and morphology on the properties of materials. Co_3O_4 with different morphologies such as nanorods, nanotubes, nanoboxes, nanocubes, and mesoporous structures have been prepared in literatures [8,21–25]. Various synthesis routes of spinel Co_3O_4 have been proposed, such as thermal deposition (300–400 °C), chemical spray pyrolysis (350–450 °C), chemical vapor deposition (CVD, 550 °C), hydrothermal method (160 °C) [26–29]. All of these methods need relatively high processing temperatures, thus the production of nanocrystalline Co_3O_4 is difficult and inconvenient. In addition to these, another limitation of most reported methods is the necessity of post-reaction thermal treatment to the materials for increasing the crystallinity, however the process always leads to particle aggregation and uncontrolled crystal growth [30].

Herein, we report a simple approach to synthesize highly dispersed Co_3O_4 nanocubes by direct precipitation of Co(II) aqueous

* Corresponding authors.
E-mail addresses: zhaojz@hnu.edu.cn, zhao_jingzhe@163.com (J. Zhao).

1385-8947/$ – see front matter © 2010 Elsevier B.V. All rights reserved.
doi:10.1016/j.cej.2010.10.080

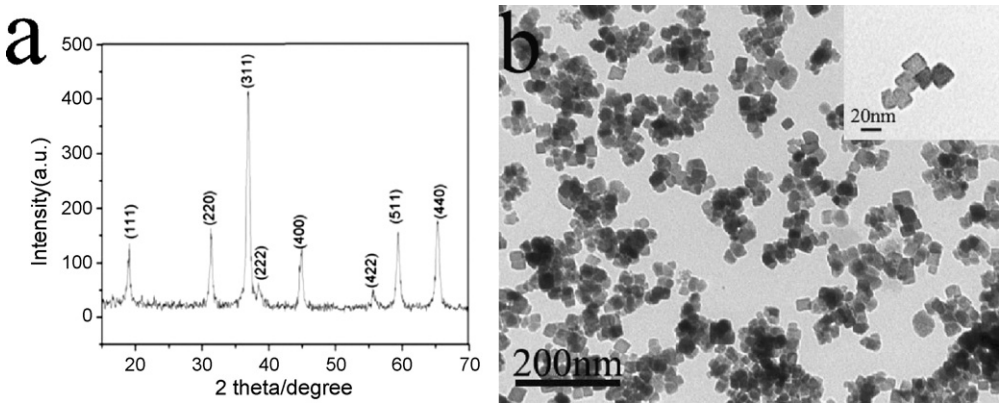

Fig. 1. Structural and morphological characterization of Co_3O_4 nanocubes prepared at 90 °C for 5 h: (a) XRD pattern; (b) TEM image. The inset in (b) is a magnified image.

solution under alkaline and oxidizing conditions at low temperatures. In this work, highly dispersed Co_3O_4 nanocubes can be obtained under a wide range of reaction parameters. The nanoparticles are stable both on morphology and dispersion status whether they are powders or dispersed suspensions. The combination of the as-prepared Co_3O_4 nanocubes with PbO_2 as electrode material extended improved electrocatalytic activities and decreased oxygen evolution potential as compared to blank PbO_2, so they could be used as potential electrode materials or electrocatalytic materials in future applications.

2. Experimental

2.1. Synthesis

In our typical synthesis, 40 mL of 0.005 M sodium oleate (SOA) and 40 mL of 0.25 M cobalt acetate ($Co(CH_3COO)_2{\cdot}4H_2O$) were mixed together and stirred in a water bath of 90 °C. After a certain volume of 0.75–3 M $NH_3{\cdot}H_2O$ was added into the above mixture, 7.5 mL of 1.35% hydrogen peroxide (H_2O_2) was dripped into the reaction system. The homogeneous solution was dynamoelectronically stirred for ten minutes while the original pink color aqueous solution gradually turned into black suspension. The color change of the liquids indicated the oxidation of Co(II) to Co(III) and formation of Co_3O_4 particles in solution by the uptake of H_2O_2. The reaction time was 3–48 h, and afterwards the liquid was removed from water bath and allowed to be filtrated. The Co_3O_4 nanocubes were obtained by washing the as-prepared precipitates several times with distilled water and then drying them under oven for hours at 60 °C.

2.2. Characterization

The shape and size of the Co_3O_4 nanocubes were characterized using a transmission electron microscope (TEM, JEOL-1230). The crystallographic structure and part information on the chemical composition of the Co_3O_4 nanocubes were identified by powder X-ray diffraction (XRD) using a Shimadzu model XRD-6000 with Cu Kα radiation. The infrared (IR) spectra were recorded on a Nicolet 5PC FTIR spectrometer using KBr pellets. UV–vis absorption spectroscopy measurements for the Co_3O_4 nanocubes were carried out on Bluestar Plus spectrometer using ethanol as a reference solvent.

3. Results and discussion

3.1. Structural and morphological characteristics

Phase identification of the as-prepared Co_3O_4 powder was determined by X-ray diffraction. Fig. 1a shows XRD pattern of the representative samples prepared. All the diffraction peaks can be indexed as cubic Co_3O_4, which match well with literature results (JCPDS No. 42-1467). No peaks from other phases were detected, indicating the pure phase of the sample. Morphological characterization of the sample is displayed in Fig. 1b. A large quantity of uniform Co_3O_4 nanocubes can be observed in the TEM image. Closer inspection of the sample (inset of Fig. 1b) reveals that those nanocubes possess average size of less than 20 nm and most of nanocubes exist as small aggregates by side attachment of nanocubes to lower the surface energy. The size of aggregates is in the range of 100–200 nm. Dispersing experiment results gave us information that steady suspensions of the Co_3O_4 nanocubes in water or ethanol could be preserved for months without obvious change, which prove excellent dispersibility of the samples.

The formation of Co_3O_4 is also confirmed with its fingerprint IR absorptions. Fig. 2 shows the IR spectrum of the sample synthesized in the presence of SOA. The strong absorption peaks at 665 cm^{-1} and 573 cm^{-1} identify the formation of Co_3O_4 [31]. The broad band centered at 3393 cm^{-1} and the peak at 1652 cm^{-1} is assigned to O–H stretching and bending modes of water. The absorptions centered at 2920 cm^{-1} are assigned to C–H stretching vibrations from SOA.

3.2. Possible reaction mechanism

Based on the analysis results, we knew that a facile aqueous method was improved to generate Co_3O_4 nanoparticles with

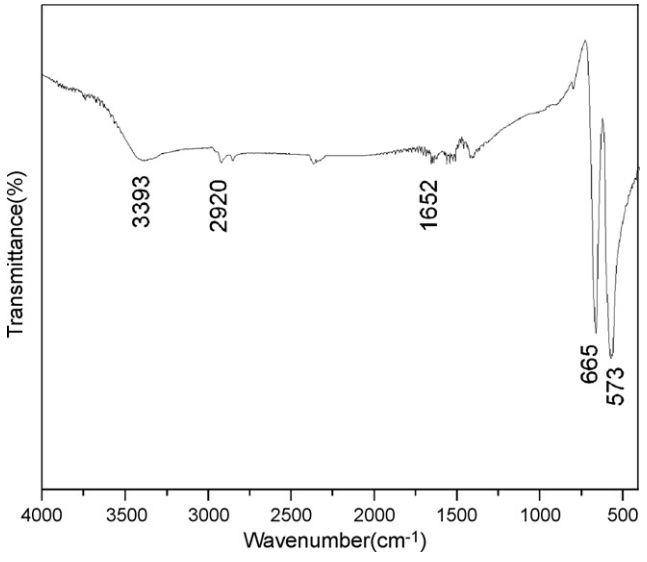

Fig. 2. IR spectrum of the Co_3O_4 nanocubes synthesized in the presence of SOA.

good dispersibility at normal atmospheric pressure and low temperature. In this simple procedure, the reaction was going with several color changes in aqueous system, from pink at the initial stage through dark-blue, brown to dark in the end. Therefore we can judge the stages of the reaction by combining their distinctive colors (see Supporting Information Fig. S1). From XRD results of dried powders, which were derived from distinguishing stages with different colors, we conclude that the whole reaction process from Co(II) to Co_3O_4 can be described as follows: First, pink $[Co(H_2O)_6]^{2+}$ combined with hydroxide ions in solution to form dark-blue precipitates of $Co(OH)_2$ in few seconds at 90 °C after pouring alkaline solution into $Co(CH_2COO)_2$ solution. Secondly, when oxidizing agent (hydrogen peroxide) was dropped into the above mixture solution, dark-blue precipitates transformed through brown CoOOH to Co_3O_4 nanoparticles in several hours. XRD results of the dried powders in different stages can prove our deduction, as shown in Fig. 3. When the reaction time was 1 h, the precipitate was Rhombohedral-phase CoOOH (JCPDS No. 14-0673) as shown in the inset of Fig. 3 [32]. Cubic-phase Co_3O_4 with less crystallization formed at reaction time of 3 h (Fig. 3). With prolonged reaction time from 3 h to 5 h (Fig. 3), Co_3O_4 crystallized well with narrow peak and increased peak intensity in the pattern. Samples prepared in enough long reaction time as 48 h also revealed crystal structure of Co_3O_4 instead of Co_2O_3 (Fig. 3). The corresponding TEM micrographs of the four samples were given in Fig. 4, which reveal the morphology variation of particles during the reaction process. Particle sizes are about 20 nm, keeping similar from 1 h to 48 h no matter what the crystal structures of the samples are, while dispersibility status and morphology change a little (see inserted images of Fig. 4 from a to d). From the overview images of Fig. 4, we can see the sample Co_3O_4 of 5 h shows the best

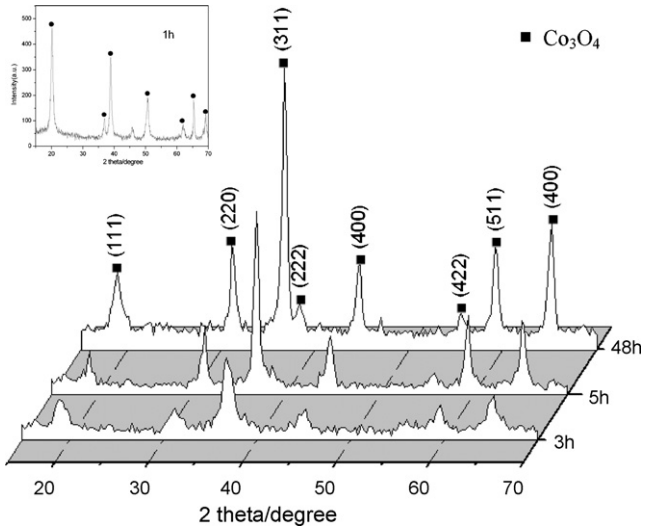

Fig. 3. XRD patterns of samples derived in different reaction time. The reaction time is 1 h (inset), 3 h, 5 h and 48 h, respectively.

dispersibility with predominant cubic morphology. A quasi-cubic structure of the precursor CoOOH reveals a self-template process in our strategy for the evolution of Co_3O_4 cubes. Compared to sample of 5 h (Fig. 4c), Co_3O_4 particles obtained in shorter (Fig. 4b) and longer (Fig. 4d) reaction time tended to form larger aggregates in some scales. This result can be confirmed by the dispersing experiments of sample powders in water or ethanol medium. The aggregation of Co_3O_4 particles in shorter reaction time should arise

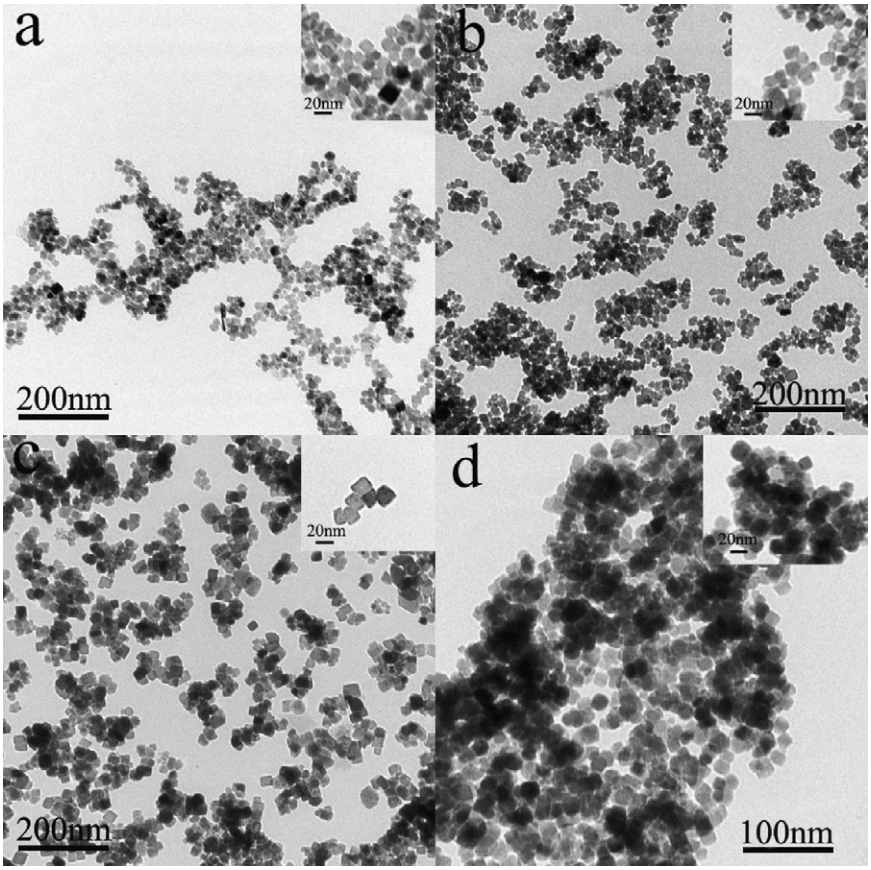

Fig. 4. TEM micrographs of samples derived in different reaction time and insets are the corresponding images with high magnification. From (a) to (d), the reaction time is 1 h, 3 h, 5 h and 48 h in turn.

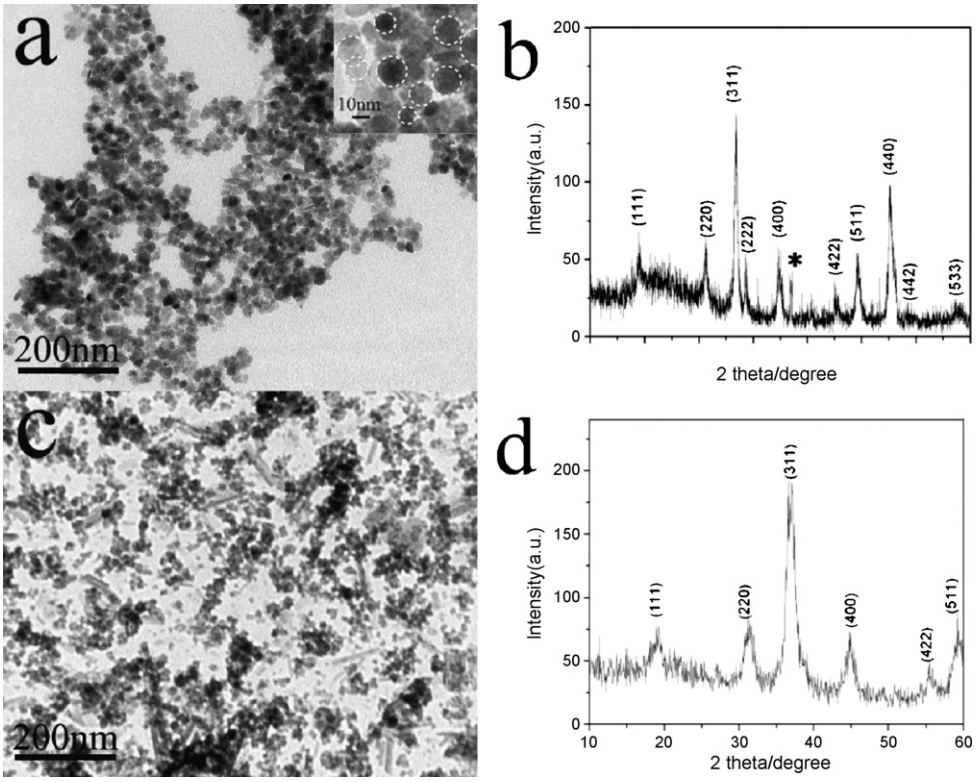

Fig. 5. Morphological and structural characterization of the Co_3O_4 sample prepared using NaOH (a, b) and urea (c, d) as precipitator. (a) and (c) are TEM images and (b) and (d) are XRD patterns, inset in (a) is the corresponding TEM images with high magnification.

from the dispersibility status of CoOOH and weak crystallization of Co_3O_4 particles. Crystal growth between Co_3O_4 nanocubes led to combined aggregates in longer reaction time [33]. Therefore, in order to achieve Co_3O_4 with excellent dispersibility, appropriate reaction time should be controlled.

3.3. Reaction parameters effect

Experiments with varied reaction parameters were performed systematically to inspect the key factors for the preparation of Co_3O_4 nanocubes.

If using NaOH or urea instead of $NH_3{\cdot}H_2O$ as the precipitator in the reaction procedure, on controlling paralleled parameters, we can find that the reactions slowed in some extent. Fig. 5a and b shows the image and crystal structure of Co_3O_4 powders with NaOH as the precipitator, in which 2 M NaOH was used to adjust pH value of the primary solution to be 8–9 and the reaction time was 5 h at 90 °C. The TEM image of the product shown in Fig. 5a displays that Co_3O_4 particles were formed in large scale with relatively good dispersion. High magnification TEM image inserted in Fig. 5a further gives us precise information that they are quasi-spherical in morphology with average diameter of less than 20 nm. XRD pattern of the sample (Fig. 5b) reveals that they are Co_3O_4 in cubic phase (JCPDS 42-1467), but there is a weak peak located at 47.1° (signed with *) which was estimated to impurity other than Co_3O_4, CoO or CoOOH. Irregular Co_3O_4 nanoplatelets were also obtained with concentrated NaOH of 5 M as precipitator in the reaction (see Supporting Information Fig. S2). When 50 mL of 2 M urea solution was substituted for ammonia as precipitator in the process, the reaction did not happen immediately even at temperature of 90 °C. Because the pH value of the primary solution was 6.0 at the beginning, Co(II) would not precipitate immediately. Precipitator as OH^- appeared in solution only when urea was heated at 90 °C for a while and afterwards precipitation happened. There were few precipitates appeared in solution when the reaction took place at 90 °C for 5 h. This revealed that the formation of Co_3O_4 slowed down in a large scale with urea as precipitator instead of $NH_3{\cdot}H_2O$. We prolonged the reaction time to 10 h in order to obtain the objective products, the terminal point of the reaction was determined on observing the faded color of the filtrate. The morphological characterization of the sample is given in Fig. 5c, a large quantity of Co_3O_4 nanoparticles are accompanied by some nanorods and nanoflakes of tens of nanometers. Fig. 5d of XRD pattern shows the pure phase of the sample. All the diffraction peaks are indexed to cubic phase Co_3O_4 (JCPDS 42-1467). From these results, we can conclude that the variety of precipitator strongly influences the morphology of the objective materials.

Temperature-dependent experiments were done by manipulating the reaction temperature from 25 °C to 90 °C. The experimental phenomena showed that at temperature lower than 70 °C we cannot obtain Co_3O_4 as products. Co_3O_4 phase appears when the temperature was increased to be higher than 70 °C. The intensities of all Co_3O_4 peaks in XRD detection were enhanced with an increase of the reaction temperature, which means that the crystallinity of Co_3O_4 gets higher. XRD results of the samples prepared at different temperatures are shown in Fig. 6a. Further TEM detection to the Co_3O_4 samples of 70 °C and 90 °C gave us results that sample of 90 °C (Fig. 1d) preserves obvious cubic-like structure compared with sample of 70 °C (Fig. 6b) with the situation of similar particle sizes of the two samples. The sample of 70 °C has similar morphology to the sample prepared in shorter reaction time (such as 3 h, see Fig. 4b), which reveals that shorter reaction time and lower reaction temperature resulted in less crystallization of samples, which is also manifested by the unobvious cubic appearance of the samples. In our strategy, we select the reaction temperature to be 90 °C for achieving better crystallized Co_3O_4 with perfect cubic morphology.

Furthermore, we investigate the effects of the concentration of reagents, the amount and type of surfactants (SOA,

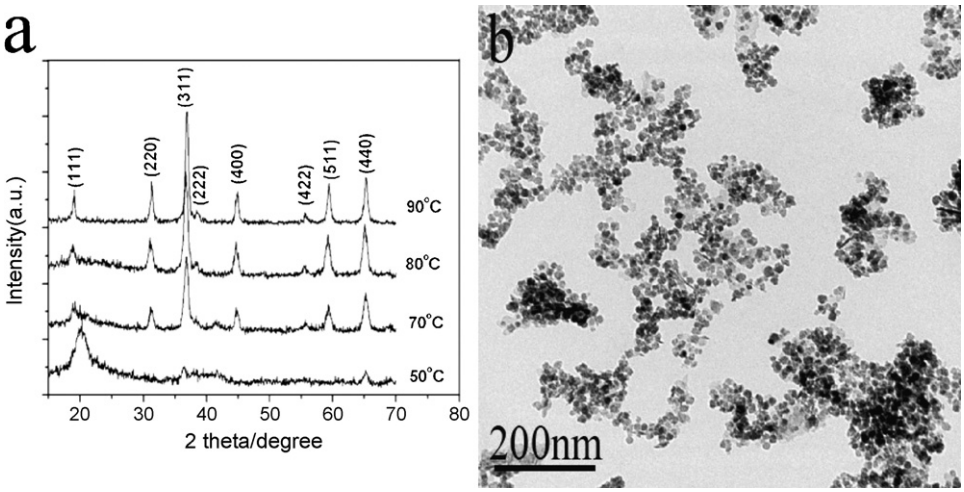

Fig. 6. XRD patterns of the as-synthesized products obtained at different reaction temperatures (a), and TEM micrograph of the sample of 70 °C (b).

polyvinylpyrrolidone (PVP), sodium dodecyl sulfate (SDS), hexadecyltrimethylammonium bromide (CTAB)) taking ammonia as precipitator. According to the results of the experiments, we found that these reaction parameters had little effect on the morphology and particle size of final products (see Supporting Information Fig. S3). Hence, we can obtain highly dispersed Co_3O_4 samples under a relatively wider range of reaction parameters.

3.4. Application performances

3.4.1. Suspension properties

In order to directly inspect the suspension properties of samples, we dispersed our samples into water by ultrasonic treatment and kept them untouched for time. Fig. 7 gives the dispersing pictures of samples modified with four different surfactants (from left to right, the surfactant used is SOA, PVP, SDS and CTAB in turn) in distilled water on dependence of preserving time. All the suspensions of the four samples present good dispersing status even after 3 months' time. This is beneficial to the applications of samples in the filed of optics and electrochemistry.

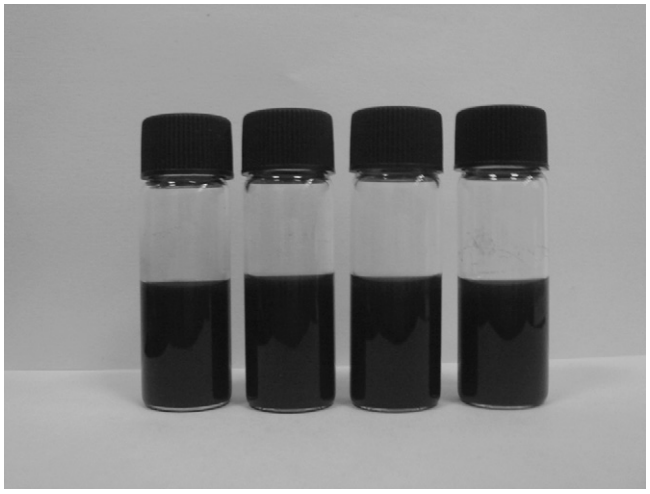

Fig. 7. Dispersing pictures of samples prepared with different surfactants in distilled water on dependence of preserving time. In picture from left to right, the dispersed samples are modified with SOA (3%), PVP (3%), SDS (3%), CTAB (3%) in turn for 3 months.

3.4.2. Optical properties

Optical absorption property of the typical SOA modified Co_3O_4 nanocubes was investigated at room temperature by UV–vis spectroscopy (Fig. 8a), two absorption peaks appear in the wavelength ranges of 200–300 nm and 350–550 nm. As has been investigated in the literatures [4,34,35], the first band gap can be assigned to O^{2-}–Co^{2+} charge transfer process while the second one concerns O^{2-}–Co^{3+} charge transfer. Co_3O_4 is a p-type semiconductor and the absorption band gap E_g can be determined by the following equation:

$$\alpha h\nu = K(h\nu - E_g)^n \quad (1)$$

where $h\nu$ is the photo energy, α is the absorption coefficient, K is a constant relative to the material, and n is either 1/2 for a direct transition or 2 for an indirect transition. Here n is 1/2 for Co_3O_4 sample. The plot of $(\alpha h\nu)^2$ versus $h\nu$ is shown in Fig. 8b. The value of $h\nu$ extrapolated to $\alpha = 0$ gives an absorption band gap energy E_g. Two absorption peaks in Fig. 8a give two E_g values for the sample. The determined E_g for the Co_3O_4 nanocubes (~20 nm) prepared in the present work is 1.77 and 3.37 eV (ΔE_g = 1.6 eV).

3.4.3. Electrocatalytic activities

In order to characterize electrocatalytic activities of the samples, steady-state current density-potential experiments were performed using combined Co_3O_4 particles and PbO_2 powders as electrodes through an electrochemical deposition route. The molar ratio of Co_3O_4 to PbO_2 is 1:100. Here we chose typical Co_3O_4 nanocubes (SOA as surfactant) and PVP induced Co_3O_4 particles as examples to characterize the electrocatalytic activities. Fig. 9 shows the steady-state current density-potential curves in 1 mol/L of NaOH electrolyte while the electrode materials contain Co_3O_4 particles with two modifications, electrode of blank PbO_2 powder was also used for comparison. Compared with the initial potential for oxygen evolution of 0.65 V on blank PbO_2 powder electrode, the potentials are reduced to 0.57 V and 0.53 V derived from Fig. 9b and c on the electrodes of combined oxides of Co_3O_4 and PbO_2, the presence of small amounts of Co_3O_4 in electrodes greatly decreased oxygen evolution potentials, thus improved the electrocatalytic activities of the electrodes. Electrode with 3% SOA modified Co_3O_4 nanocubes (Fig. 9c) exhibits higher electrocatalytic activity than the one with 3% PVP modified Co_3O_4 particles (Fig. 9b), even though the two Co_3O_4 samples have similar morphology and particle size. This reveals that surface status of Co_3O_4 nanocubes influences electrochemical properties of electrode materials.

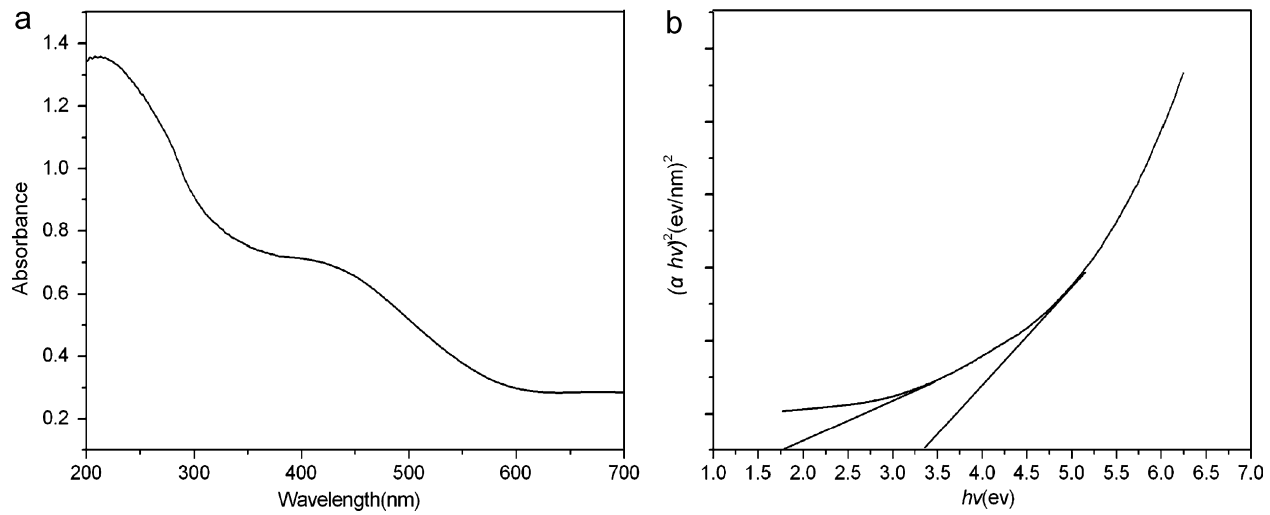

Fig. 8. (a) UV–vis absorption spectrum of the typical Co_3O_4 nanocubes in the presence of 3 wt% SOA, (b) plot of $(\alpha h\nu)^2$ versus $h\nu$ evaluated from data in Fig. 8a.

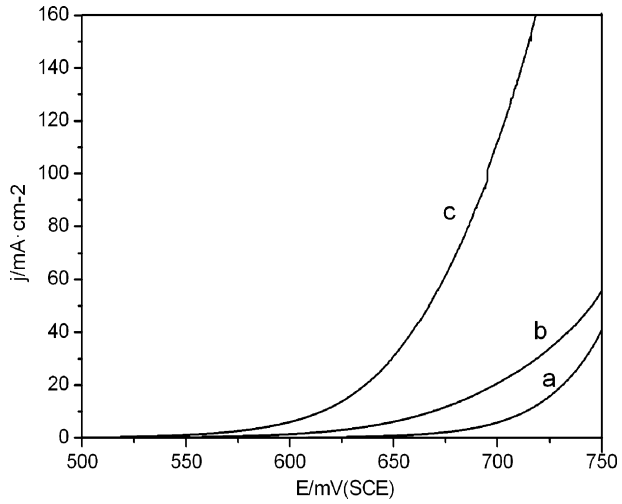

Fig. 9. Steady-state current density–potential curves in 1 mol/L NaOH on electrodes containing blank PbO_2 (a) and combined oxides of PbO_2 and Co_3O_4 (b, c). Electrode materials: (a) PbO_2, (b) $PbO_2 + Co_3O_4$ (3% PVP), (c) $PbO_2 + Co_3O_4$ (3% SOA).

4. Conclusions

We have demonstrated a facile synthesis of highly dispersed Co_3O_4 nanocubes in aqueous phase at low temperature. The nanometer Co_3O_4 powers were directly precipitated from Co(II) aqueous solution under alkaline and oxidizing conditions. Co_3O_4 nanocubes can be achieved under a wide range of reaction parameters, which can be preserved as stable suspension in aqueous and ethanol medium for several months. Appropriate reaction time and temperature should be controlled to get better crystallized Co_3O_4 nanocubes with perfect cubic appearance and good dispersibility. $NH_3{\cdot}H_2O$ as precipitator is essential to achieve cubic-like Co_3O_4 particles. Electrodes containing Co_3O_4 nanocubes with varied modification all show perfect electrocatalytic activities compared to blank PbO_2, thus they can be used as potential electrode materials or electrocatalytic materials.

Acknowledgments

This work was supported by National Program on Key Basic Research Project (973 Program) (Grant No. 2007CB310503), Science and Technology Project of Changsha City (Grant No. k0905033-11) and also supported by the National Natural Science Foundation of China (Grant No. J0830415).

Appendix A. Supplementary data

Supplementary data associated with this article can be found, in the online version, at doi:10.1016/j.cej.2010.10.080.

References

[1] C.N.R. Rao, A.K. Cheetham, Science and technology of nanomaterials: current status and future prospects, J. Mater. Chem. 11 (2001) 2887–2894.
[2] B.B. Lakshmi, P.K. Dorhout, C.R. Martin, Sol–gel template synthesis of semiconductor nanostructures, Chem. Mater. 9 (1997) 857–862.
[3] Y.D. Li, M. Sui, Y. Ding, G.H. Zhang, J. Zhuang, C. Wang, Preparation of $Mg(OH)_2$ nanorods, Adv. Mater. 12 (2000) 818–821.
[4] S.W. Chen, J.M. Sommers, Alkanethiolate-protected copper nanoparticles: spectroscopy, electrochemistry, and solid-state morphological evolution, J. Phys. Chem. B 105 (2001) 8816–8820.
[5] R. Xu, H.C. Zeng, Self-generation of tiered surfactant superstructures for one-pot synthesis of Co_3O_4 nanocubes and their close- and non-close-packed organizations, Langmuir 20 (2004) 9780–9790.
[6] M.P. Pileni, Nanocrystal self-assemblies: fabrication and collective properties, J. Phys. Chem. B 105 (2001) 3358–3371.
[7] T. He, D. Chen, X.L. Jiao, Controlled synthesis of Co_3O_4 nanoparticles through oriented aggregation, Chem. Mater. 16 (2004) 737–743.
[8] R. Xu, H.C. Zeng, Mechanistic investigation on salt-mediated formation of free-standing Co_3O_4 nanocubes at 95 °C, J. Phys. B 107 (2003) 926–930.
[9] G. Furlanetto, L. Formaro, Precipitation of spherical Co_3O_4 particles, J. Colloid Interface Sci. 170 (1995) 169–175.
[10] S.K. Tripathy, M. Christy, N.H. Park, E.K. Suh, S. Anand, Y.T. Yu, Hydrothermal synthesis of single-crystalline nanocubes of Co_3O_4, Mater. Lett. 62 (2008) 1006–1009.
[11] J.H. He, T.H. Wu, C.L. Hsin, K.M. Li, L.J. Chen, Y.L. Chueh, Beaklike SnO_2 nanorods with strong photoluminescent and field-emission properties, Small 2 (2006) 116–120.
[12] L.P. Xu, S. Sithambaram, Y.S. Zhang, C.H. Chen, L. Jin, R. Joesten, S.L. Suib, Novel urchin-like CuO synthesized by a facile reflux method with efficient olefin epoxidation catalytic performance, Chem. Mater. 21 (2009) 1253–1259.
[13] C.C. Hu, Y.T. Wu, K.H. Chang, Low-temperature hydrothermal synthesis of Mn_3O_4 and MnOOH single crystals: determinant influence of oxidants, Chem. Mater. 20 (2008) 2890–2894.
[14] J. Zhou, Y. Ding, S.Z. Deng, L. Gong, N.S. Xu, Z.L. Wang, Three-dimensional tungsten oxide nanowire networks, Adv. Mater. 17 (2005) 2107–2110.
[15] M. Casas-Cabanas, G. Binotto, D. Larcher, A. Lecup, V. Giordani, J.M. Tarascon, Defect chemistry and catalytic activity of nanosized Co_3O_4, Chem. Mater. 21 (2009) 1939–1947.
[16] W.Y. Li, L.N. Xu, J. Chen, Co_3O_4 nanomaterials in lithium-ion batteries and gas sensors, Adv. Funct. Mater. 15 (2005) 851–857.
[17] Y.G. Li, B. Tan, Y.Y. Wu, Mesoporous Co_3O_4 nanowire arrays for lithium ion batteries with high capacity and rate capability, Nano Lett. 8 (2008) 265–270.
[18] X.W. Lou, D. Deng, J.Y. Lee, L.A. Archer, Self-supported formation of needlelike Co_3O_4 nanotubes and their application as lithium-ion battery electrodes, Adv. Mater. 20 (2008) 258–262.

[19] K. Ramachandram, C.O. Oriakhi, M.M. Lemer, V.R. Koch, Intercalation chemistry of cobalt and nickel dioxides: a facile route to new compounds containing organocations, Mater. Res. Bull. 31 (1996) 767–772.
[20] E.L. Salabas, A. Rumplecker, F. Kleitz, F. Radu, F. Schuth, Exchange anisotropy in nanocasted Co_3O_4 nanowires, Nano Lett. 6 (2006) 2977–2981.
[21] G.X. Wang, X.P. Shen, J. Horvat, B. Wang, H. Liu, D. Wexler, J. Yao, Hydrothermal synthesis and optical, magnetic, and supercapacitance properties of nanoporous cobalt oxide nanorods, J. Phys. Chem. C 113 (2009) 4357–4361.
[22] N Du, H. Zhang, B.D. Chen, J.B. Wu, X.Y. Ma, Z.H. Liu, Y.Q. Zhang, D.R. Yang, X.H. Huang, J.P. Tu, Porous Co_3O_4 nanotubes derived from $Co_4(CO)_{12}$ clusters on carbon nanotube templates: a highly efficient material for Li-battery applications, Adv. Mater. 19 (2007) 4505–4509.
[23] L.H. Zhuo, J.C. Ge, L.H. Cao, B. Tang, Solvothermal synthesis of CoO, Co_3O_4, $Ni(OH)_2$ and $Mg(OH)_2$ nanotubes, Cryst. Growth Des. 9 (2009) 1–6.
[24] T. He, D.R. Chen, X.L. Jiao, Y.L. Wang, Co_3O_4 nanoboxes: surfactant-templated fabrication and microstructure characterization, Adv. Mater. 18 (2006) 1078–1082.
[25] A. Rumplecker, F. Kleitz, E.L. Salabas, F. Schuth, Hard templating pathways for the synthesis of nanostructured porous Co_3O_4, Chem. Mater. 19 (2007) 485–496.
[26] C. Pirovano, S. Trasatti, The point of zero charge of Co_3O_4: effect of preparation procedure, J. Electroanal. Chem. 180 (1984) 171–184.
[27] D.Y. Kim, S.H. Ju, H.Y. Koo, S.K. Hong, Y.C. Kangf, Synthesis of nanosized Co_3O_4 particles by spray pyrolysis, J. Alloys Compd. 417 (2006) 254–258.
[28] A.U. Mane, K. Shalini, A. Wohlfart, A. Devi, S.A. Shivashankar, Strongly oriented thin films of Co_3O_4 deposited on single-crystal MgO(1 0 0) by low-pressure, low-temperature MOCVD, J. Cryst. Growth 240 (2002) 157–163.
[29] L.L Li, Y. Chu, Y. Liu, J.L. Song, D. Wang, X.W. Du, A facile hydrothermal route to synthesize novel Co_3O_4 nanoplates, Mater. Lett. 62 (2008) 1507–1510.
[30] M.E. Baydi, G. Poillerat, J.L. Rehspringer, J.L. Gautier, J.F. Koenig, P. Chartier, A sol–gel route for the preparation of Co_3O_4 catalyst for oxygen electrocatalysis in alkaline medium, J. Solid State Chem. 109 (1994) 281–288.
[31] T. He, D.R. Chen, X.L. Jiao, Y.L. Wang, Y.Z. Duan, Solubility-controlled synthesis of high-quality Co_3O_4 nanocrystals, Chem. Mater. 17 (2005) 4023–4030.
[32] J.H. Yang, T. Sasaki, Synthesis of CoOOH hierarchically hollow spheres by nanorod self-assembly through bubble templating, Chem. Mater. 20 (2008) 2049–2056.
[33] M. Rycenga, J.M. Mclellan, Y.N. Xia, Controlling the assembly of silver nanocubes through selective functionalization of their faces, Adv. Mater. 20 (2008) 2416–2420.
[34] F. Gu, C.Z. Li, Y.J. Hu, L. Zhang, Synthesis and optical characterization of Co_3O_4 nanocrystals, J. Cryst. Growth 304 (2007) 369–373.
[35] Y.G. Zhang, Y.C. Chen, T. Wang, J.H. Zhou, Y.G. Zhao, Synthesis and magnetic properties of nanoporous Co_3O_4 nanoflowers, Micropor. Mesopor. Mater. 114 (2008) 257–261.